

# Complexity and Performance Tradeoffs of Near-Optimal Detectors for Cooperative ISI Channels

Yanjie Peng, Kai Zhang, Andrew G. Klein, *Member, IEEE*, and Xinming Huang, *Senior Member, IEEE*  
 Department of Electrical and Computer Engineering  
 Worcester Polytechnic Institute  
 Worcester, MA 01609

**Abstract**—Cooperative communication has attracted a lot of attention for its ability to exploit increased spatial diversity available at distributed antennas on other nodes in the system. For a cooperative system employing non-orthogonal amplify-and-forward half-duplex relays, the maximum likelihood sequence estimation (MLSE) is the optimal detector in intersymbol interference (ISI) channels. The implementation complexity of the optimal detector scales exponentially with the length of effective channel impulse response (CIR), however, which becomes very long and sparse as the relay period increases. In this paper, we focus on suboptimal detector design, complexity, and performance for cooperative relays in ISI channels. We first explore use of a decision feedback sequence estimator (DFSE). Next, to exploit the structured sparsity in the effective CIR, we consider an iterative belief propagation (BP) algorithm based detector. Using simulation results, we explore the tradeoff between complexity and performance.

**Index Terms**—Cooperative communications, sparse fading channel, decision feedback sequence estimation, belief propagation algorithm.

## I. INTRODUCTION

Recently, cooperative diversity [1], [2] and relay networks [3] have attracted a lot of attention for their ability to exploit increased spatial diversity available at distributed antennas on other nodes in the system. Here, we consider a system where a half-duplex relay employs the non-orthogonal amplify-and-forward (AF) protocol for the case when the channels exhibit frequency selectivity or intersymbol interference (ISI). Several previous works have investigated detector design for such a situation where relays aid transmission through ISI channels. In [4] it was shown that, for a cooperative system with one amplify-and-forward relay node, the effective channel impulse response (CIR) becomes periodically time-varying due to the half-duplex operation of the relay. An optimal maximum-likelihood sequence estimation (MLSE) detector realization based on the Viterbi algorithm (VA) was presented; however, the implementation was shown to be limited by high computational complexity which increases exponentially with the length of the effective CIR. Since the duration of the effective CIR is extended as the relay period increases, the use of optimal MLSE becomes impractical even when the relay period has just a few symbol durations. It was shown in [5] that the effective CIR becomes long and sparse when the relay

period increases. By exploiting the sparse characteristic of the effective CIR, a near-optimal detector based on a multitrellis Viterbi algorithm (MVA) was proposed which decomposed the original trellis into multiple parallel irregular sub-trellises by investigating the dependencies between the received symbols. For the MVA-based detector, if the dependencies are appropriately simplified, it was shown that the complexity does not depend on the length of the effective CIR but only on the number of non-zero coefficients. However, the simplification of the dependencies is not straightforward for an effective CIR with an arbitrary structure of non-zero tap coefficients. Also, irregular sub-trellises increase the implementation overhead compared to a regular trellis as in traditional MLSE.

In this paper, two alternative detectors are proposed to achieve a balance between the computational complexity and performance. The first detector is based on a decision feedback sequence estimation (DFSE) [6], [7], which is a popular scheme for ISI channels which are too long for MLSE to be practical. The other detector we propose is based on the belief propagation (BP) [8]–[10] algorithm and is specifically designed for the sparse effective CIR encountered in our model. Traditionally these two detectors are used with fixed, static channels. In our model, however, the effective channel in the cooperative communications is periodically time-varying, even when the component channels themselves are static. Consequently, the detectors we propose are modified, as appropriate, to account for this. Through simulations in frequency selective fading channels, we will demonstrate the uncoded performance of these detectors when compared to the optimal MLSE detector. In addition to quantifying the performance of these detectors, we will also include an analysis of the implementation complexity as well as a discussion on complexity/performance tradeoffs.

## II. SYSTEM MODEL IN ISI CHANNELS

The cooperative system with one relay node is shown in Fig. 1. Both source and relay have only one antenna. We consider a system where a source transmits a continuous stream of data to a destination, and a simplistic AF half-duplex relay assists the source by amplifying and forwarding the data to the destination. Since the channels from source and

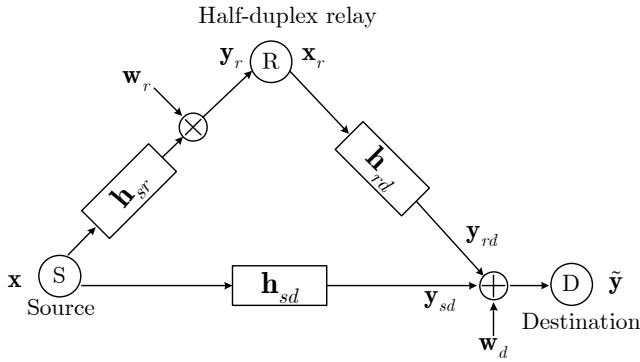


Fig. 1. System model

relay to destination are statistically independent, the three-node cooperative communication scheme effectively forms spatial diversity. The relay period  $T$  is a parameter which defines the frame structure where the relay receives for  $T$  symbol periods, and then transmits for  $T$  symbol periods. The relay repeats these two tasks alternately. Note that since our focus is the detector design, we do not consider specific coding schemes and channel estimation in our model, and thus the perfect channel knowledge is assumed for the detector.

The source sends the symbols  $\mathbf{x} = [x[0], \dots, x[N-1]]^T \in \mathbb{C}^N$ , where  $N$  is the number of transmitted symbols. Considering the effects of pulse shaping, we adopt equivalent discrete-time channel models [11] with complex additive white Gaussian noise (AWGN). The equivalent source-destination, source-relay, and relay-destination channel impulse responses are denoted by  $\mathbf{h}_{sd}$ ,  $\mathbf{h}_{sr}$ ,  $\mathbf{h}_{rd}$ , respectively, and they have corresponding channel lengths  $L_{sd}$ ,  $L_{sr}$  and  $L_{rd}$  (e.g.  $\mathbf{h}_{sd} = [h_{sd}[0], h_{sd}[1], \dots, h_{sd}[L_{sd}-1]]^T$ ). The signals  $\mathbf{w}_r$  and  $\mathbf{w}_d$  are AWGN at the relay and the destination with variance  $\sigma_r^2$  and  $\sigma_d^2$ , respectively.

The destination receives the superposition of the two signals from the source and the relay, and the received signal can be expressed as

$$\begin{aligned}
 \tilde{\mathbf{y}} &= \mathbf{y}_{sd} + \mathbf{y}_{rd} + \mathbf{w}_d \\
 &= \mathbf{H}_{sd}\mathbf{x} + \mathbf{H}_{rd}\mathbf{x}_r + \mathbf{w}_d \\
 &= \mathbf{H}_{sd}\mathbf{x} + \mathbf{H}_{rd}\mathbf{\Gamma}\mathbf{y}_r + \mathbf{w}_d \\
 &= \mathbf{H}_{sd}\mathbf{x} + \mathbf{H}_{rd}\mathbf{\Gamma}(\mathbf{H}_{sr}\mathbf{x} + \mathbf{w}_r) + \mathbf{w}_d \\
 &= \underbrace{(\mathbf{H}_{sd} + \mathbf{H}_{rd}\mathbf{\Gamma}\mathbf{H}_{sr})}_{\triangleq \tilde{\mathbf{H}}}\mathbf{x} + \underbrace{(\mathbf{H}_{rd}\mathbf{\Gamma}\mathbf{w}_r + \mathbf{w}_d)}_{\triangleq \tilde{\mathbf{w}}}
 \end{aligned}$$

where  $\mathbf{H}_{sd} \in \mathbb{C}^{(N+L_{sd}-1) \times N}$  is the complex Toeplitz channel convolution matrix defined by  $[\mathbf{H}_{sd}]_{i,j} = h_{sd}[i-j]$ ,  $1 \leq i, j$  and  $0 \leq i-j \leq L_{sd}-1$ . The Toeplitz channel matrices  $\mathbf{H}_{rd} \in \mathbb{C}^{(N+L_{sr}+L_{rd}-2) \times (N+L_{sr}-1)}$  and  $\mathbf{H}_{sr} \in \mathbb{C}^{(N+L_{sr}-1) \times N}$  are defined in the same way as  $\mathbf{H}_{sd}$ ,  $\mathbf{y}_r \in \mathbb{C}^{N+L_{sr}-1}$  is the signal received by the relay, and  $\mathbf{x}_r \in \mathbb{C}^{N+L_{sr}-1}$  is the signal transmitted from the relay. Note that for the matrix dimensions to be compatible, we require that  $L_{sd} = L_{sr} + L_{rd} - 1$ ; if this is not satisfied, we can append zeros to the appropriate matrix without loss of generality. The

function of  $\mathbf{\Gamma} \in \mathbb{C}^{(N+L_{sr}-1) \times (N+L_{sr}-1)}$  is to impose the half-duplex constraint by selecting groups of  $T$  symbols from  $\mathbf{y}_r$  (receiving), scaling these symbols by a factor  $\beta$  (amplifying), and then delaying the scaled symbols of  $\mathbf{y}_r$  for transmission in the next  $T$  symbol block (forwarding). The value of  $\beta$  is typically chosen to satisfy an average power constraint at the relay by choosing  $\beta = \sqrt{\frac{P_r}{\|\mathbf{h}_{sr}\|^2 P_s + \sigma_r^2}}$  where  $P_s$  and  $P_r$  are the source power and relay power respectively. The constant matrix  $\mathbf{\Gamma}$  is given by

$$\mathbf{\Gamma} \triangleq \beta \mathbf{I}_{(N+L_{sr}-1)} \otimes \begin{bmatrix} \mathbf{0}_{T \times T} & \mathbf{0}_{T \times T} \\ \mathbf{I}_{T \times T} & \mathbf{0}_{T \times T} \end{bmatrix} \quad (1)$$

where  $\otimes$  denotes Kronecker product. Here we implicitly require that  $N + L_{sr} - 1$  be divisible by  $2T$ .

Note that  $\tilde{\mathbf{w}}$  is colored, not white, since the AWGN on the source-relay link is amplified-and-forwarded over the relay-destination ISI channel which colors the noise. To whiten the noise, we factor the noise covariance matrix as [12]:

$$\mathbf{G}\mathbf{G}^H = \sigma_d^2 \mathbf{I} + \sigma_r^2 \mathbf{H}_{rd} \mathbf{\Gamma} \mathbf{\Gamma}^H \mathbf{H}_{rd}^H \quad (2)$$

which can be accomplished by taking  $\mathbf{G}$  to be the Cholesky factorization of the covariance. After applying the whitening filter to the received signal, the whitening filter output becomes

$$\begin{aligned}
 \mathbf{y} &= \mathbf{G}^{-1} \tilde{\mathbf{H}} \mathbf{x} + \mathbf{G}^{-1} \tilde{\mathbf{w}} \\
 &= \mathbf{H} \mathbf{x} + \mathbf{w}
 \end{aligned} \quad (3)$$

where  $\mathbf{w}$  is now *white* Gaussian noise. Note that the effective whitened channel matrix  $\mathbf{H}$  has a block Toeplitz structure with rows repeating every multiple of  $2T$  due to the operation of half-duplex relay [4]. It can be interpreted as a periodically time-varying FIR channel which consists of  $2T$  sets of different CIR as  $\mathbf{h}_0, \mathbf{h}_1, \dots, \mathbf{h}_{2T-1}$ , where  $\mathbf{h}_0 = [h_0[0], h_0[1], \dots, h_0[L-1]]^T$ ,  $\mathbf{h}_1 = [h_1[0], h_1[1], \dots, h_1[L-1]]^T, \dots$ , and  $L$  is the length of effective CIR.  $L$  can be lower bounded in terms of the constituent channel lengths and the relay period as

$$L = \max(L_{sd}, L_{sr} + L_{rd} + T - 1). \quad (4)$$

After applying the whitening filter, the equivalent system model in the absence of noise is shown in Fig. 2. Assuming that at time  $n$ , the corresponding coefficients of the periodically time-varying effective CIR are

$$\mathbf{h}_n = \mathbf{h}_{\text{mod}(n, 2T)} \in \{\mathbf{h}_0, \mathbf{h}_1, \dots, \mathbf{h}_{2T-1}\}, \quad n = 0, 1, \dots \quad (5)$$

where  $\text{mod}(\cdot)$  is the modulus.

An optimal MLSE scheme based on a modified Viterbi algorithm is proposed in [4] to deal with the periodically time-varying channels induced by the half-duplex relay. Similar to the traditional MLSE, the implementation cost of such a detector for cooperative system increases exponentially with respect to the length of effective CIR  $L$ . In practice, it is likely that the relay period  $T$  is chosen to be very long, possibly spanning hundreds of symbols, so that the relay is not required to switch frequently between transmit and receive modes. When the relay period  $T$  is long, the effective channel length

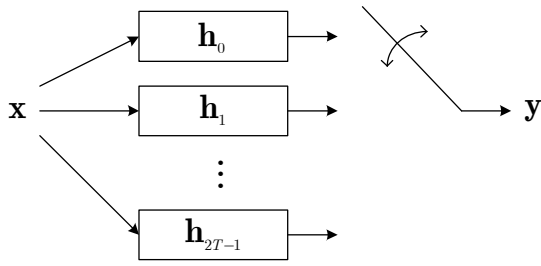


Fig. 2. Equivalent system model in the absence of noise

$L$  becomes large according to (4). In addition, as we will discuss in Section IV, the channel also becomes sparse as  $T$  is increased. A direct implementation of the traditional Viterbi algorithm becomes impractical for large values of  $T$  expected to be encountered in practice. Consequently, this raises the need for near-optimal detectors with reduced complexity that are well-suited to the long, sparse structure of the effective CIR.

### III. DFSE-BASED DETECTOR

A considerable amount of research has been undertaken to exploit reduced complexity detectors for long ISI channels. A well-known approach is linear decision feedback detectors [13] which have low complexity. Another approach is to truncate the CIR to a short length, and use a decision feedback equalizer to cancel the residual ISI before the processing of Viterbi detector [14]. However, both schemes suffer from error propagation due to incorrect decision feedback. In [6], [7], DFSE is proposed to incorporate the decision feedback mechanism within the calculation of branch metric directly in the Viterbi detector to enhance the reliability of the feedback decision.

#### A. DFSE detector model

In the trellis of DFSE, each state provides only partial information about the actual state of the channel. The states describe all possible values taken on by a small number  $\mu < L$  of previous inputs. The required residual information is provided by a built-in decision feedback in branch metric computations. The traditional DFSE is modified and incorporated in the scenario of cooperative communications. In the branch metric calculation, the ideal received signal at time  $n$  is given by

$$s[n] = \sum_{i=0}^{\mu-1} h_n[i]x[n-i] + \underbrace{\sum_{i=\mu}^{L-1} h_n[i]\tilde{x}[n-i]}_{\text{Residual ISI}} \quad (6)$$

where  $(x[n], \dots, x[n-\mu+1])$  in the first sum are determined by the state in the trellis, and  $(\tilde{x}[n-\mu], \dots, \tilde{x}[n-L+1])$  in the second sum are the estimate of the partial state extracted from the survivor path leading to that state. This estimate is used to cancel ISI from symbols greater than  $\mu$  symbol periods in the past. The residual ISI from the remaining  $L-\mu$  symbols is canceled by the per-survivor decision feedback [15].

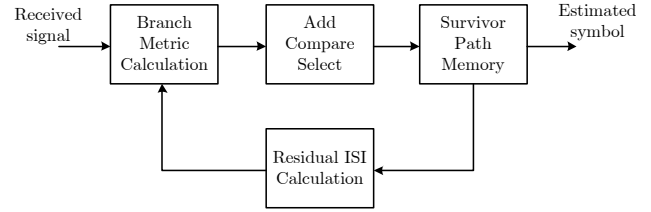


Fig. 3. DFSE block diagram

Note that (6) is modified to tackle the time-varying channel indicated in (5). The coefficients adopted by the decision feedback filter also change with a period of  $2T$ . The complexity can be managed by varying  $\mu$ , the number of ISI symbol used in the trellis. If  $\mu = L$ , the algorithm is equivalent to Viterbi algorithm; if  $\mu = 1$ , the algorithm reduces to the zero-forcing DFE. Choosing appropriate  $\mu$  enables the DFSE to achieve a good tradeoff between performance and complexity.

#### B. DFSE detector architecture

The block diagram is shown in Fig. 3. The branch metric calculation unit calculates the Euclidean distance between the received signal and estimated signal along the trellis path. Then the add-compare-select unit recursively computes path metrics and decision bits. The path metric for each state is updated for the next iteration, and the decision indicating the survivor path are recorded and retrieved from the survivor-path memory unit in order to estimate the transmitted symbols. In the meanwhile, the survivor path information leading to each state is extracted and feed back to the branch metric calculation unit.

#### C. Complexity analysis

The complex multipliers used in branch metric calculation and residual ISI calculation dominate the whole computational complexity. Consider a cooperative communication system using BPSK modulation. In the branch metric calculation, the number of states is  $2^{\mu-1}$ , and there are 2 branch metric calculations for each state. Thus the number of complex multipliers used in branch metric calculation is  $2^\mu$ . For the residual ISI calculation, there is a  $(L-\mu)$ -length decision feedback filter for each possible state transition, requiring  $(L-\mu)2^\mu$  complex multipliers. The total computational complexity with respect to the number of complex multipliers is  $(L-\mu+1)2^\mu \sim \mathcal{O}(2^\mu)$ .

### IV. BELIEF PROPAGATION-BASED DETECTOR

DFSE can be applied as a suboptimal detector scheme for a wide class of long ISI channel in cooperative systems. However, it is interesting to point out that a large relay period  $T$  makes the effective CIR become sparse. The reason for this is that, at the destination, the contribution from the AF relay “looks” like a multipath arrival with a path delay roughly equal to  $T$ . As  $T$  grows large, the length of the effective CIR also grows, and additionally becomes sparse; this effect is described in more detail in [5].

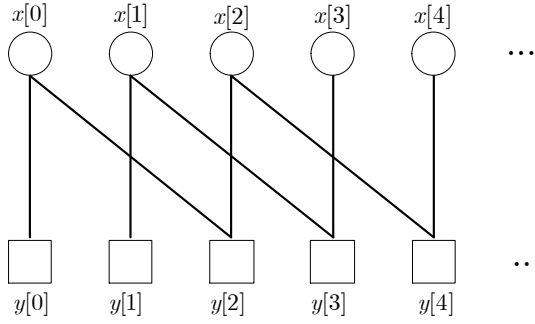


Fig. 4. Factor graph of an example channel  $[h[0], 0, h[2]]^T$

Detectors specifically for sparse channels have been investigated previously. The parallel trellis Viterbi algorithm (PTVA) proposed in [16] reformulated the original single trellis into a set of independent trellises. These independent trellises operate in parallel and have less overall complexity than a single trellis. The PTVA requires that the channel have equi-spaced coefficients, however, which cannot be satisfied in our case. In our previous work [5], a near-optimal detector is proposed based on the MVA algorithm [17]. For the MVA-based detector, the complexity does not depend on the length of CIR but only on the number of non-zero coefficients if a certain subset of dependencies is neglected. However, the simplification of the dependencies is not straightforward for an effective CIR with general structure. Furthermore, irregular sub-trellises increase the implementation overhead compared to a regular trellis as in traditional MLSE.

The belief propagation algorithm provides an alternative solution to the sparse channel detection problem. The BP algorithm has been widely used in iterative decoding of LDPC codes on a factor graph [18]. It has also been used for detection over ISI channels [8]–[10] since the input-output relationship of an ISI channel can be represented as a factor graph. For example, Fig. 4 shows the factor graph of a CIR  $[h[0], 0, h[2]]^T$ . Input symbols and output signals of the ISI channel are described as the variable nodes (circle) and check nodes (square) on the factor graph respectively. The connections (edges) between the variable nodes and the check nodes represent dependencies of input and output. For example,  $y[3]$  is connected to  $x[1]$  and  $x[3]$ , since  $y[3] = h[0]x[3] + h[3]x[0] + w[3]$ , where  $w[3]$  is the additive noise.

#### A. BP detector algorithm

The BP algorithm is also called two-phase message-passing algorithm, in which check-to-variable (CTV) and variable-to-check (VTC) informations are transmitted along the edges to update each other iteratively. During the first phase, the extrinsic information is computed at the check nodes based on the known CIR coefficients and the *a priori* probability information from the variable nodes. The updated extrinsic information is then passed from each check node to its connected variable nodes. During the second phase, the variable nodes update their *a priori* information and send it

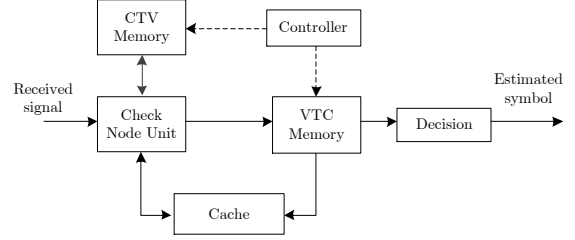


Fig. 5. Architecture diagram of the BP-based detector

back to their connected check nodes. The same procedure is repeated iteratively. After several iterations, the variable nodes are accumulated with sufficient likelihood information and a hard decision can be made for each input bit. The detailed operations of the BP algorithm are summarized as follows:

1) *Calculating CTV information:* The extrinsic information at check node  $n$  for variable node  $n - j$ ,  $j = 0, 1, \dots, L - 1$  is computed as (7), where  $\mathbf{D} = \{x[n - L + 1], \dots, x[n - 1], x[n]\}$ ,  $b[n] = \frac{x[n] + 1}{2}$  for BPSK and  $Q_{n-i \rightarrow n}$  is the *a priori* information calculated at the variable node  $n - i$  for check node  $n$ . The nonlinear log-sum-exponential function in (7) could be implemented with look-up tables (LUTs), but it is not desirable because the LUTs would require a large size memory. As a good approximation, the calculation in (7) can be simplified as (8) by Jacobian logarithm with negligible performance loss [19]. Unlike the factor graph of fixed channels, since the effective CIR in cooperative communication is periodically time-varying, the connections along the factor graph do not maintain the same pattern. Accordingly, the calculation of extrinsic information must adopt different coefficients depending on the node index  $n$ , i.e. the channel coefficients used in  $R_{n \rightarrow n - j}$  are  $\mathbf{h}_n = \mathbf{h}_{\text{mod}(n, 2T)} \in \{\mathbf{h}_0, \mathbf{h}_1, \dots, \mathbf{h}_{2T-1}\}$ .

2) *Calculating VTC information:* Upon receiving the updated extrinsic information from the check nodes, the variable nodes update the *a priori* information for the next iteration. The *a priori* information at variable node  $n$  for check node  $n + j$  is calculated as

$$Q_{n \rightarrow n+j} = \sum_{i=0, i \neq j}^{L-1} R_{n+i \rightarrow n} \quad (9)$$

3) *Summing up and decision:* After several iterations of message passing, the overall likelihood for the transmitted symbol is

$$\Lambda_n = \sum_{i=0}^{L-1} R_{n+i \rightarrow n} = Q_{n \rightarrow n+j} + R_{n+j \rightarrow n} \quad (10)$$

Based on the accumulated log-likelihood value of each variable node, a hard decision on  $x[n]$  can be made for each symbol.

$$R_{n \rightarrow n-j} = \log \frac{\sum_{\forall \mathbf{D}: x[n-j]=+1} \exp \left\{ \frac{-|y[n] - \sum_{i=0}^{L-1} h_n[i] x[n-i]|^2}{2\sigma^2} + \sum_{i=0, i \neq j}^{L-1} b[n-i] Q_{n-i \rightarrow n} \right\}}{\sum_{\forall \mathbf{D}: x[n-j]=-1} \exp \left\{ \frac{-|y[n] - \sum_{i=0}^{L-1} h_n[i] x[n-i]|^2}{2\sigma^2} + \sum_{i=0, i \neq j}^{L-1} b[n-i] Q_{n-i \rightarrow n} \right\}} \quad (7)$$

$$\approx \max_{\forall \mathbf{D}: x[n-j]=+1} \left\{ \frac{-|y[n] - \sum_{i=0}^{L-1} h_n[i] x[n-i]|^2}{2\sigma^2} + \sum_{i=0, i \neq j}^{L-1} b[n-i] Q_{n-i \rightarrow n} \right\} - \max_{\forall \mathbf{D}: x[n-j]=-1} \left\{ \frac{-|y[n] - \sum_{i=0}^{L-1} h_n[i] x[n-i]|^2}{2\sigma^2} + \sum_{i=0, i \neq j}^{L-1} b[n-i] Q_{n-i \rightarrow n} \right\} \quad (8)$$

### B. BP detector architecture

We propose a low-complexity architecture for BP-based detector design. The overall architecture is shown in Fig. 5. The detector mainly consists of a check node unit (CNU) responsible for check node update, the VTC memory and CTV memory which are used to store the belief propagation messages, a cache which is a temporarily storage for the nodes currently being processed, and a controller which controls the iterative detection and the sequential processing within each iteration.

The proposed architecture is a serial architecture intended to minimize hardware resources. The CNU only processes one check node at each time that corresponds to one received signal. A pipeline architecture is implemented in the CNU design such that it can take a new signal input every clock cycle. Since the VTC calculation at the variable node is simply a sum operation, we include that as part of the CNU. The VTC memory stores the VTC information of each bit in a frame of data. The extrinsic information for a check node is stored in the CTV memory. Since the channel length  $L$  is much less than the frame length  $N$  ( $L \ll N$ ), a cache only contains the VTC information of  $L$  variable nodes that may have connection with the check node being processed. This is similar to a “sliding window” that only needs to fetch one new VTC information from the large VTC memory when CNU moves to process the next check node.

### C. Complexity analysis

The main computational complexity lies in the CNU that computes the CTV information as in (8), particularly in the computation of the Euclidean distance. Since the effective CIR is known,  $\sum_{i=0}^{L-1} h_n[i] x[n-i]$  can be simplified as a group of summations or a precalculated look-up table. In a pipeline architecture, all the Euclidean distance values must be calculated in parallel. Suppose that the number of non-zero coefficients of  $\mathbf{h}_n$  is  $L'$  ( $\ll L$ ), the number of paths required to evaluate  $\sum_{i=0}^{L-1} h_n[i] x[n-i]$  in parallel is  $2^{L'}$  for BPSK modulated symbols and each path needs one complex multiplier. In general, the computational complexity of the BP detector is  $\mathcal{O}(2^{L'})$ , which increases exponentially with the

number of non-zero coefficients of the effective CIR. Furthermore, it is important to note that more iterations will improve the performance, however, the resulting low throughput of detection would make it an inappropriate choice for high-rate application.

## V. SIMULATION RESULTS

We simulate the bit error rate (BER) performance of the detectors with the following parameters: the transmitted BPSK signal consists of i.i.d. unit-power symbols  $x[n] = \{\pm 1\}$ , the relay transmission power is  $P_r = 1$ , and the symbol frame length  $N = 500$ . The SNR values  $E_b/N_o^{(d)} = 1/\sigma_d^2$  and  $E_b/N_o^{(r)} = 1/\sigma_r^2$  denote bit-energy-to-noise ratio for the destination and the relay, respectively. Unless otherwise specified, we assume  $E_b/N_o^{(r)} = E_b/N_o^{(d)} + 10$  dB, which represents a scenario where the source-relay link is of higher quality, on average, than the source-destination link. We consider Rayleigh fading channels with  $L_{\{sd, sr, rd\}} = 2$ , and each coefficient is a zero-mean complex Gaussian random variable with unit average power. The individual channel coefficients are assumed to be statistically independent.

For the DFSE scheme,  $\mu = 2$  and  $\mu = 4$  are considered. For the BP scheme, we choose the number of iterations as 2 and 5. We also consider the MLSE as a reference curve. The BER performance for different detectors when the relay period  $T = 5$  and  $T = 10$  is shown in Fig. 6 and Fig. 7, respectively. We note that with these parameter choices, the effective CIR lengths for these two simulations are then  $L = 8$  and  $L = 13$ , respectively, according to (4).

At a BER of  $10^{-3}$ , when  $T = 5$ , the DFSE scheme exhibits performance approximately 1.3 dB away from the optimal performance when  $\mu = 2$ , and a performance penalty of 1.2 dB when  $\mu = 4$ . Recall that when  $\mu = L = 8$ , the DFSE becomes the MLSE. The BP scheme, on the other hand, performs only 0.5 dB away from optimal when 2 iterations are used, and only 0.1 dB away when 5 iterations are used. When  $T = 10$ , i.e.  $L = 13$ , the DFSE scheme shows approximately 1.2 dB and 1dB away from the optimal performance for  $\mu = 2$  and  $\mu = 4$ , respectively. While the BP scheme performs 0.5 dB and 0.05 dB away from optimal for 2 and 5 iterations, respectively.

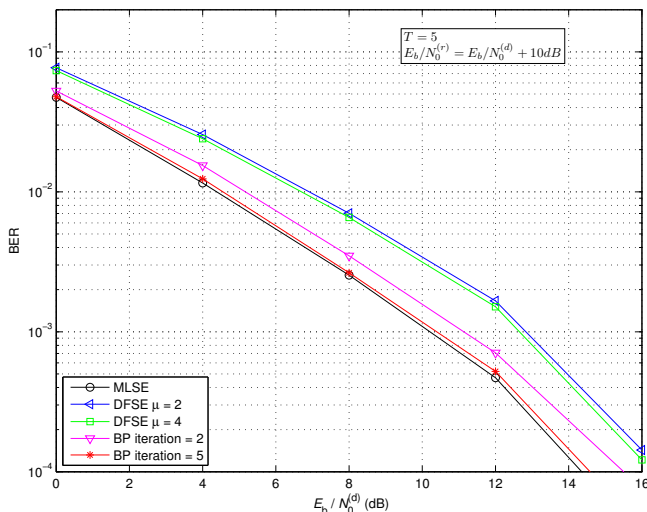


Fig. 6. BER performance for different detectors when  $T = 5$

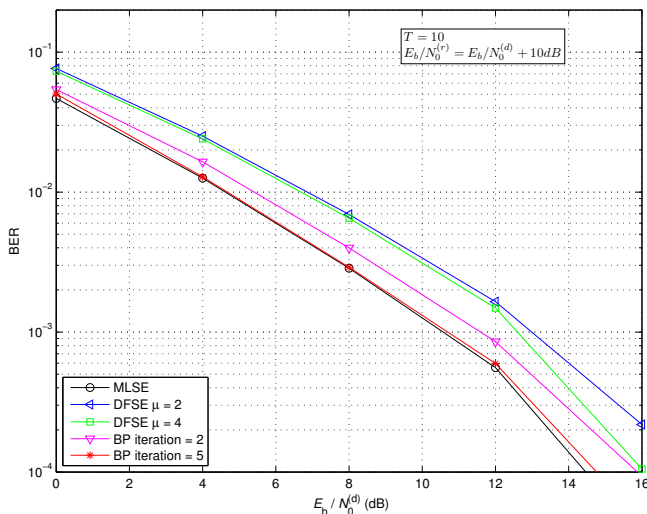


Fig. 7. BER performance for different detectors when  $T = 10$

## VI. COMPLEXITY AND PERFORMANCE TRADEOFFS

Having presented the computational complexity and performance, we now consider practical implementation issues with respect to computing resources, latency, and performance tradeoffs. The parameters used in simulations in Section V are assumed here, i.e.  $L_{\{sd, sr, rd\}} = 2$  and  $T = 10$  so that  $L = 13$ .

When an optimal MLSE detector is considered as a reference, the number of dominant computing elements (complex multipliers) is  $2^L = 2^{13}$ . Meanwhile, a DFSE-based detector consumes  $(L - \mu + 1)2^\mu = 48$  elements when  $\mu = 2$ , and 160 elements when  $\mu = 4$ . For a BP-based detector, the number of non-zero coefficients is  $L' = 6$ , so it uses up to  $2^{L'} = 64$  elements. The DFSE scheme is the most cost-saving solution among the three when  $\mu$  is small. The DFSE detector has a MLSE-like structure; thus the decoding latency, which is equal to the traceback length, is similar to MLSE. On the other hand,

the latency of the BP detector is determined by the iteration number. A large number of iterations results in low throughput for the BP detector, rendering it unsuitable for use in high-rate applications. In some situations, however, the additional performance offered by increasing the number of iterations is often minimal. We also note that if the individual channel lengths are large, there will be a significant number of non-zero taps in the effective channel, and the BP detector may be too complex. In such circumstances, the effective channel can be first equalized to a sparse target impulse response (TIR) by a partial response equalization before BP detection, which is a possible topic for future research.

## REFERENCES

- [1] A. Sendonaris, E. Erkip, and B. Aazhang, "User cooperation diversity, Parts I & II," *IEEE Trans. Commun.*, vol. 51, Nov. 2003.
- [2] J. N. Laneman, D. N. C. Tse, and G. W. Wornell, "Cooperative diversity in wireless networks: Efficient protocols and outage behavior," *IEEE Trans. Inf. Theory*, vol. 50, no. 12, pp. 3062–3080, Dec. 2004.
- [3] G. Kramer, M. Gastpar, and P. Gupta, "Cooperative strategies and capacity theorems for relay networks," *IEEE Trans. Inf. Theory*, vol. 51, pp. 3037–3063, Sep. 2005.
- [4] Y. Peng, A. G. Klein, and X. Huang, "Design of a maximum-likelihood detector for cooperative communications in intersymbol interference channels," in *Proceedings of the 19th ACM Great Lakes symposium on VLSI*. ACM New York, NY, USA, May 2009, pp. 429–432.
- [5] —, "Detector design for half-duplex relay networks in ISI channels," in *IEEE Military Communications Conference, 2009. MILCOM 2009*, Oct 2009, pp. 1–7.
- [6] A. Duel-Hallen and C. Heegard, "Delayed decision-feedback sequence estimation," *IEEE Trans. Commun.*, vol. 37, no. 5, pp. 428–436, 1989.
- [7] M. V. Eyuboglu and S. U. H. Qureshi, "Reduced-state sequence estimation with set partitioning and decision feedback," *IEEE Trans. Commun.*, vol. 36, no. 1, pp. 13–20, 1988.
- [8] M. N. Kaynak, T. M. Duman, and E. M. Kurtas, "Belief propagation over frequency selective fading channels," in *Proc. VTC2004-Fall Vehicular Technology Conference 2004 IEEE 60th*, vol. 2, Sep. 26–29, 2004, pp. 1367–1371.
- [9] G. Colavolpe and G. Geremi, "On the application of factor graphs and the sum-product algorithm to isi channels," *IEEE Trans. Commun.*, vol. 53, no. 5, pp. 818–825, May 2005.
- [10] S. Roy, T. M. Duman, and V. K. McDonald, "Error rate improvement in underwater mimo communications using sparse partial response equalization," *IEEE J. Ocean. Eng.*, vol. 34, no. 2, pp. 181–201, Apr. 2009.
- [11] P. Hoher, "A statistical discrete-time model for the wss multipath channel," *IEEE Trans. Veh. Technol.*, vol. 41, no. 4, pp. 461–468, 1992.
- [12] G. Forney Jr, "Maximum-likelihood sequence estimation of digital sequences in the presence of intersymbol interference," *IEEE Trans. Inf. Theory*, vol. 18, no. 3, pp. 363–378, May 1972.
- [13] J. Proakis, *Digital Communications*, 4th ed. New York: McGraw-Hill, 2000.
- [14] W. Lee and F. Hill, "A maximum-likelihood sequence estimator with decision-feedback equalization," *IEEE Trans. Commun.*, vol. 25, no. 9, pp. 971–979, 1977.
- [15] R. Raheli, A. Polydoros, and C.-K. Tzou, "Per-survivor processing: a general approach to mlse in uncertain environments," *IEEE Trans. Commun.*, vol. 43, no. 234, pp. 354–364, Feb. 1995.
- [16] N. C. McGinty, R. A. Kennedy, and P. Hoher, "Parallel trellis Viterbi algorithm for sparse channels," *IEEE Commun. Lett.*, vol. 2, no. 5, pp. 143–145, May 1998.
- [17] N. Benvenuto and R. Marchesani, "The Viterbi algorithm for sparse channels," *IEEE Trans. Commun.*, vol. 44, no. 3, pp. 287–289, Mar. 1996.
- [18] H.-A. Loeliger, "An introduction to factor graphs," *IEEE Signal Process. Mag.*, vol. 21, no. 1, pp. 28–41, Jan. 2004.
- [19] P. Robertson, E. Villebrun, and P. Hoher, "A comparison of optimal and sub-optimal MAP decoding algorithms operating in the log domain," in *1995 IEEE International Conference on Communications, 1995. ICC'95 Seattle, Gateway to Globalization*, vol. 2, 1995.